Journal of Science and Technology in Civil Engineering, HUCE, 2026, 20 (4): 35–50

CALCULATION OF GEOMETRIC PROPERTIES FOR STORAGE RACK COLUMN SECTIONS

Bui Hung Cuong[a], Nguyen Dinh Hoa[a,*], Nguyen Quang Khai[b], Dinh Van Thuat[a], Benoit P. Gilbert[c]

[a]*Faculty of Building and Industrial Construction, Hanoi University of Civil Engineering, 55 Giai Phong road, Bach Mai ward, Hanoi, Vietnam*
[b]*Consultancy Company of University of Civil Engineering (CCU), Hanoi University of Civil Engineering, 55 Giai Phong road, Bach Mai ward, Hanoi, Vietnam*
[c]*School of Engineering and Built Environment - Civil and Environmental Engineering, Griffith University, 170 Kessels Road Brisbane, Queensland, Australia*

Article history:
Received 15/6/2026, Revised 15/7/2026, Accepted 03/8/2026, Available online 16/10/2026, Version of Record 25/12/2026

Abstract

This paper develops closed-form analytical formulas for calculating the geometric properties of open-section thin-walled steel storage rack columns, with particular emphasis on flexural-torsional buckling analysis. The study focuses on storage rack columns, which are typically fabricated from cold-formed thin-walled steel and have complex cross-sectional geometries including folded edges, lips, and stiffeners. The theoretical formulation is based on Vlasov thin-walled beam theory, in which cross-sectional warping is described by sectorial coordinates. On this basis, warping constant and shear-center location of the section are derived. Numerical examples validate the proposed formulas through comparison with CUFSM and GBTUL results, and the calculated geometric properties are subsequently used to evaluate the flexural-torsional buckling capacity of the members.

Keywords: storage rack column; thin-walled member; flexural-torsional buckling; sectorial properties; closed-form formula.

1. Introduction

Steel storage rack systems used to store goods storage are common in industrial warehouses, distribution centers, and modern logistics facilities. In such structural systems, storage rack columns are the primary load-bearing members; they receive and transfer vertical loads from stored goods and also resist lateral actions arising during service through semi-rigid beam-to-column connections.

To meet requirements for flexible assembly, reduced self-weight, and efficient material utilization, storage rack columns are commonly fabricated from cold-formed thin-walled steel with open cross sections. These sections often have complex geometries, including several folded edges and stiffeners. Such geometric characteristics make the global buckling behavior of storage rack columns more complex than that of conventional steel sections.

For storage rack column sections, the determination of geometric properties like shear center or warping constant using simple analytical formulas remains limited because of their complex cross-sectional shapes. In design practice and research, these properties are usually obtained using specialized software such as CUFSM [1] and Thin-Wall-2 [2], or through computational programs developed

*Corresponding author. *E-mail address:* hoand@huce.edu.vn (Hoa, N. D.)
https://doi.org/10.31814/stce.huce2026-20(4)-03 p-ISSN 1859-2996; e-ISSN 2734-9268
© 2026 The Author(s). Published by Hanoi University of Civil Engineering. Licensed under CC BY-NC-ND 4.0.



Figure 1. Typical storage rack columns

from the general formulations of Cuong [3] and Xiang [4]. However, when a specific section must be checked rapidly, the preparation of detailed geometric input data and reliance on specialized software may be inconvenient for design engineers, especially during preliminary design or when many section alternatives need to be investigated. At present, AISI [5] provides analytical formulas for calculating the geometric properties of cold-formed thin-walled members, but these formulas are limited to lipped channel sections. Based on Vlasov thin-walled beam theory [6], general analytical expressions have been presented for simple open sections such as channel and I-sections. Gil-Martin [7] also used Vlasov theory to investigate sectorial coordinates of thin-walled member sections and to determine their properties from sectorial coordinates. Lue [8] proposed and presented a numerical procedure for evaluating the geometric properties of arbitrary open thin-walled sections; however, the formulation is applied to discretized straight-line elements of the section, and therefore the calculation may be time-consuming for complex sections with many bends. Shama [9] discussed the sectorial properties of simple open thin-walled sections such as C, I, and T-sections. In addition, Freitas et al. [10] and the design standard [11] have addressed the analysis and verification of storage rack columns; nevertheless, explicit analytical formulas for calculating the geometric properties of these section types have not yet been provided. In Vietnam, studies have been conducted on the calculation of geometric properties of thin-walled members, including Quyen [12] for channel section and Tuyen and Cuong [13] for closed sections. Furthermore, Tung and Cuong [14] limited their derivation to the geometric properties of welded built-up I-sections. However, the addition of inward or outward intermediate lips in these specific rack columns significantly complicates the sectorial coordinate diagram and shifts the shear center. This leaves a clear gap for direct algebraic solutions for these multi-stiffened profiles.

In response to this need, the present study focuses on establishing closed-form formulas for calculating the geometric properties that include shear center and warping constant of gross sections while accounting for flexural-torsional buckling. The theoretical basis of the study is Vlasov thin-walled beam theory, in which characteristic quantities such as the shear center and warping constant are determined directly from the geometric dimensions of the section. The proposed formulas enable rapid evaluation of the geometric properties required for capacity for global buckling and reduce dependence on specialized computational software. The results provide a convenient calculation tool that can be applied to the design, verification, and optimization of storage rack column sections in thin-walled steel storage rack systems. The study calculated the geometric properties using the developed equations and compared the results with those obtained from numerical software. In addition, these geometric properties were employed in the calculation of the flexural-torsional buckling capacity of rack columns. This buckling capacity analysis directly demonstrates the practical application and necessity of the derived sectorial parameters (a_x and I_w) in structural design practice.

2. Theory of open thin-walled members

Vlasov thin-walled beam theory [6] extends conventional bending theory by accounting for warping deformation of open sections through the sectorial coordinate, denoted by ω.

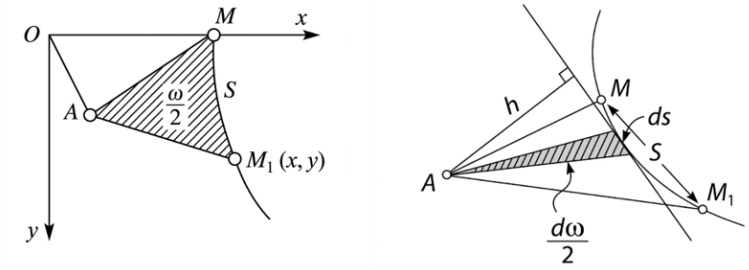


Figure 2. Sectorial coordinate along the median line of an open thin-walled section

For a pole A and a selected origin M on the section median line in Fig. 2, the sectorial coordinate at point M_1 (with arc length s) is defined as:

$$\omega = \int_0^s d\omega \tag{1}$$

where $d\omega$ is the differential sectorial coordinate. If h is the perpendicular distance from A to the tangent to the median line, then $d\omega = h.ds$ and

$$\omega = \int_0^s h.ds \tag{2}$$

Based on this coordinate system, the sectorial geometric properties of the cross section (with differential area dF) are defined by the following integrals:

Sectorial static moment:

$$S_\omega = \int_F \omega dF \tag{3}$$

Sectorial product of inertia:

$$I_{\omega x} = \int_F \omega y dF \tag{4}$$

$$I_{\omega y} = \int_F \omega x dF \tag{5}$$

Warping constant:

$$I_\omega = \int_F \omega^2 dF \tag{6}$$

The shear center and the principal pole are determined from the conditions that both the sectorial static moment and the sectorial product of inertia vanish:

$$S_\omega = 0; \quad I_{\omega x} = 0; \quad I_{\omega y} = 0$$

Assume that the shear center is $A_0\,(x_{A_0}, y_{A_0})$ with a_x, a_y denoting the distances along the x- and y-axes between points A and A_0. Then:

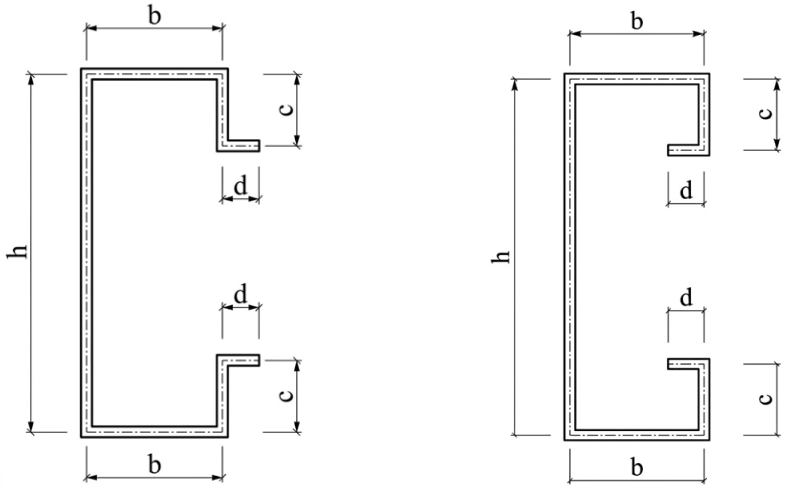
$$a_x = x_{A_0} - x_A = \frac{I_{\omega_A x}}{I_x} \tag{7}$$

$$a_y = y_{A_0} - y_A = \frac{I_{\omega_A y}}{I_y} \tag{8}$$

where I_x, I_y are the moments of inertia with respect to the centroidal principal axes.

3. Analytical formulas for the geometric properties of representative storage rack sections

This study considers the two types of cold-formed lipped channel thin-walled sections in Fig. 3 used in storage rack columns, defined by the section dimensions height h, flange width b, lip length c, stiffener length d, and thickness t, with stiffeners oriented either outward or inward. The folded segments are assumed to be mutually perpendicular, as shown in Fig. 3. Additionally, the small corner radii of the sections are neglected in the derivation because they meet the EN 1993-1-3 [15] requirements ($r \leq 5t, r \leq 0.1b_p$). Therefore, the cross-sections are modeled using their median lines with sharp corners. This simplification is common in cold-formed steel analysis and has a negligible effect on the geometric properties.



(a) Channel section with outward stiffeners

(b) Channel section with inward stiffeners

Figure 3. Cold-formed lipped channel sections with outward and inward stiffeners representative of storage rack columns

For convenient identification, the two section types are denoted in this paper as follows: Outward-lipped channel section (abbreviated as OLC); Inward-lipped channel section (abbreviated as ILC)

3.1. Outward-lipped channel section (OLC)

a. Determination of the centroid of the OLC section

Assume that the coordinate origin is located as shown in Fig. 4. Then $C\,(x_c; y_c)$ is the centroid of the section, and its coordinates are determined as follows:

$$x_c = \frac{\sum_{i=1}^{7} x_i S_i}{\sum_{i=1}^{7} S i} = \frac{b^2 + 2bc + 2bd + d^2}{h + 2b + 2c + 2d};\ y_c = \frac{h}{2} \quad (9)$$

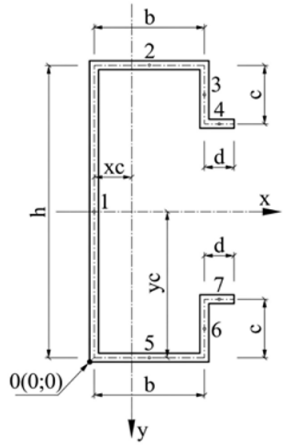
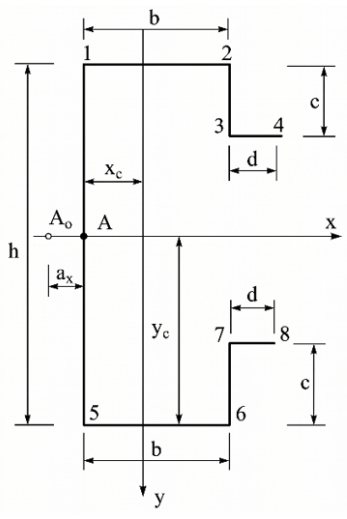


Figure 4. Outward-lipped channel section

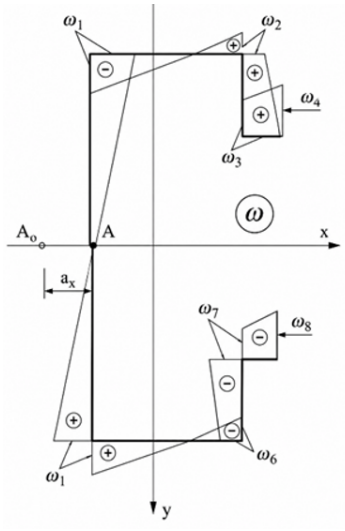
b. Determination of the moments of inertia of the OLC section

$$\begin{aligned} I_x &= \sum_{i}^{7} \left(I_{xi} + a_i d_{yi}^2\right) \\ &= \frac{th^3}{12} + 2\left(\frac{bt^3}{12} + \frac{h^2}{4}bt\right) + 2\left[\frac{tc^3}{12} + \frac{(h-c)^2}{4}ct\right] + 2\left[\frac{dt^3}{12} + \left(\frac{h}{2} - c\right)^2 dt\right] \\ &= \frac{th^3}{12} + \frac{bt^3}{6} + \frac{h^2 bt}{2} + \frac{tc^3}{6} + \frac{(h-c)^2 ct}{2} + \frac{dt^3}{6} + \frac{(h-2c)^2 dt}{2} \end{aligned} \quad (10)$$

c. Determination of the sectorial-coordinate diagram of the OLC section



(a) Sectorial-coordinate points on the section



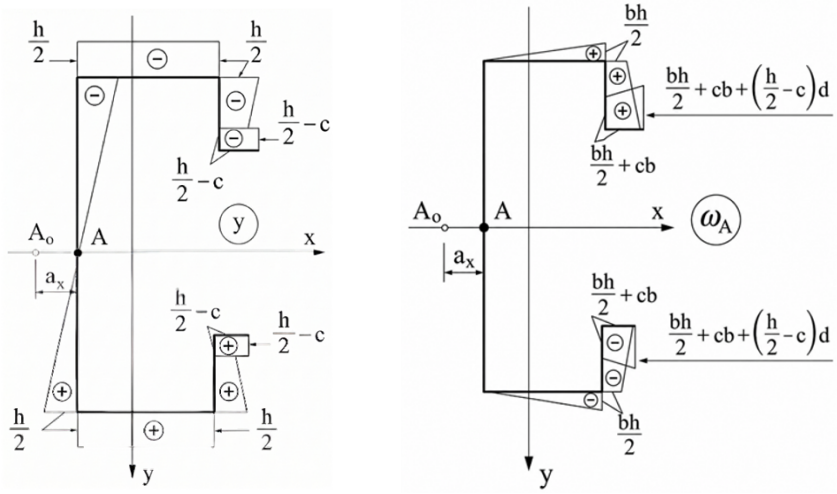
(b) Sectorial-coordinate diagram for the OLC section

Figure 5. Sectorial-coordinate diagram of the OLC section

Assume that point A is the origin, and that A_0 is the principal pole. Points 1 to 8 in Fig. 5(a) denote the sectorial coordinates at the corner locations of the section; the sectorial coordinates at these points

are calculated as follows:

$$
\begin{aligned}
\omega_A &= 0 \\
\omega_1 &= -2 \times S_{\Delta A_0 A5} = -\frac{a_x h}{2} \\
\omega_2 &= \omega_1 + 2 \times S_{\Delta A_0 56} = -\frac{a_x h}{2} + \frac{bh}{2} = -\frac{h}{2}(a_x - b) \\
\omega_3 &= \omega_2 + 2 \times S_{\Delta A_0 67} = -\frac{h}{2}(a_x - b) + c(a_x + b) \\
\omega_4 &= \omega_3 + 2 \times S_{\Delta A_0 78} = -\frac{h}{2}(a_x - b) + c(a_x + b) + \left(\frac{h}{2} - c\right)d \\
\omega_5 &= 2 \times S_{\Delta A_0 A5} = \frac{a_x h}{2} \\
\omega_6 &= \omega_5 - 2 \times S_{\Delta A_0 56} = \frac{a_x h}{2} - \frac{bh}{2} = \frac{h}{2}(a_x - b) \\
\omega_7 &= \omega_6 - 2 \times S_{\Delta A_0 67} = \frac{h}{2}(a_x - b) - c(a_x + b) \\
\omega_8 &= \omega_7 - 2 \times S_{\Delta A_0 78} = \frac{h}{2}(a_x - b) - c(a_x + b) - \left(\frac{h}{2} - c\right)d
\end{aligned}
\tag{11}
$$



(a) y-ordinate diagram (b) Sectorial-coordinate diagram ω_A

Figure 6. Diagrams of the y-ordinate and the sectorial coordinate ω_A for the OLC section

d. Determination of the sectorial product of inertia $I_{\omega_A x}$ of the OLC section

According to Eq. (4), one obtains

$$
I_{\omega_A x} = \int_F \omega_A y dF = \int_F \omega_A y t ds = \sum_{i=1}^{7} t_i \int_0^{S_i} \omega_A y ds
$$

According to Vereshchagin's graphical multiplication method, after multiplying the sectorial-coordinate diagram ω_A and the y-ordinate diagram in Fig. 6, one obtains:

$$I_{\omega_A x} = -2t\left(\frac{bh}{2}\frac{b}{2}\frac{h}{2}\right) - 2t\left[\frac{bh}{2}c\frac{h-c}{2} + \frac{cbc}{2}\left(\frac{h}{2} - \frac{2c}{3}\right)\right] - 2t\left[\frac{bh + 2cb + \left(\frac{h}{2} - c\right)d}{2}d\left(\frac{h}{2} - c\right)\right]$$

After simplifying the expression, one obtains

$$I_{\omega_A x} = -tb\left[\frac{bh^2}{4} + \frac{hc\,(h-c)}{2} + c^2\left(\frac{h}{2} - \frac{2c}{3}\right)\right] - td\left(bh + 2cb + \frac{hd}{2} - cd\right)\left(\frac{h}{2} - c\right) \tag{12}$$

e. Determination of the shear-center location of the OLC section

According to Eq. (7), the shear-center coordinates $A_0(x_{A_0}, y_{A_0})$ with a_x, a_y denoting the distances along the x- and y-axes between A and A_0 are obtained as follows:

$$a_x = \frac{I_{\omega_A x}}{I_x} \tag{13}$$

Because the x-axis is an axis of symmetry for the OLC section, one has $a_y = 0$.

f. Determination of the warping constant I_ω of the OLC section

According to Eq. (6), the warping constant of the OLC section is calculated as follows:

$$I_\omega = \int_F \omega^2 dF = \sum_{i=1}^{7} t_i \int_0^{S_i} \omega^2 ds$$

According to Vereshchagin's graphical multiplication method, after multiplying the sectorial-coordinate diagram ω in Fig. 5(b) by itself and simplifying, one obtains the following formula:

$$I_\omega = 2t\left[\begin{array}{l} \dfrac{a_x^2 h^3}{24} + \dfrac{a_x^3 h^2}{12} + \dfrac{(b-a_x)^3 h^2}{12} + (c+d)\dfrac{h^2(b-a_x)^2}{4} \\ + \left(\dfrac{c}{2} + d\right)hc\,(a_x+b)\,(b-a_x) + \left(\dfrac{c}{3} + d\right)c^2(a_x+b)^2 \\ + \dfrac{d^3}{3}\left(\dfrac{h}{2} - c\right)^2 + \dfrac{hd^2}{2}\left(\dfrac{h}{2} - c\right)(b-a_x) + d^2 c\left(\dfrac{h}{2} - c\right)(a_x+b) \end{array}\right] \tag{14}$$

3.2. Inward-lipped channel section (ILC)

a. Determination of the centroid of the ILC section

Assume that the coordinate origin is located as shown in Fig. 7. Then $C\,(x_C; y_C)$ is the centroid of the section, and its coordinates are determined as follows:

$$x_c = \frac{\sum_{i=1}^{7} x_i S_i}{\sum_{i=1}^{7} S\,i} = \frac{b^2 + 2bc + 2bd - d^2}{h + 2b + 2c + 2d}; \quad y_c = \frac{h}{2} \tag{15}$$

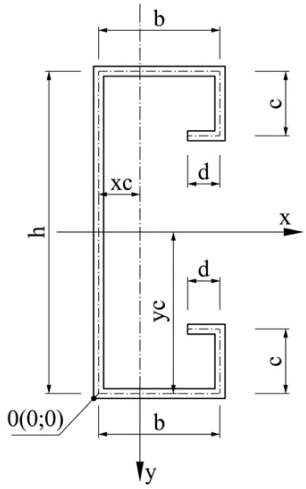


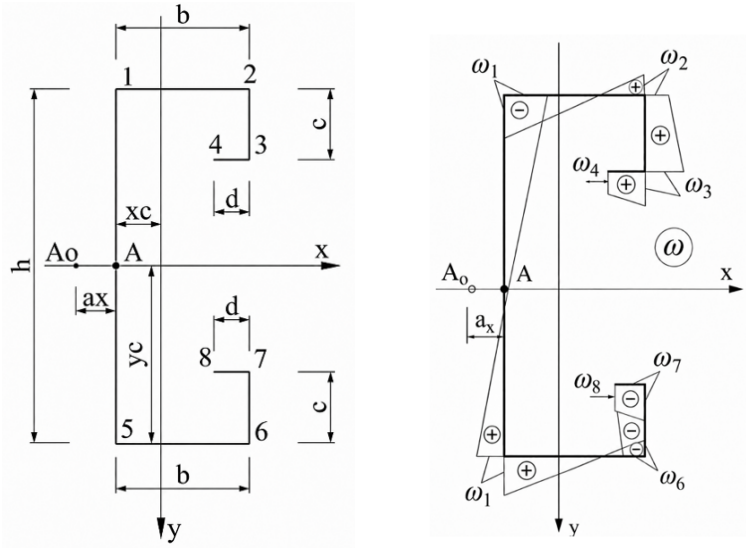
Figure 7. Inward-lipped channel section

b. Determination of the moments of inertia of the ILC section

Similar to the OLC section, the formula for the moments of inertia of the ILC section is as follows:

$$I_x = \frac{th^3}{12} + \frac{bt^3}{6} + \frac{h^2bt}{2} + \frac{tc^3}{6} + \frac{(h-c)^2ct}{2} + \frac{dt^3}{6} + \frac{(h-2c)^2dt}{2} \tag{16}$$

c. Determination of the sectorial-coordinate diagram of the ILC section



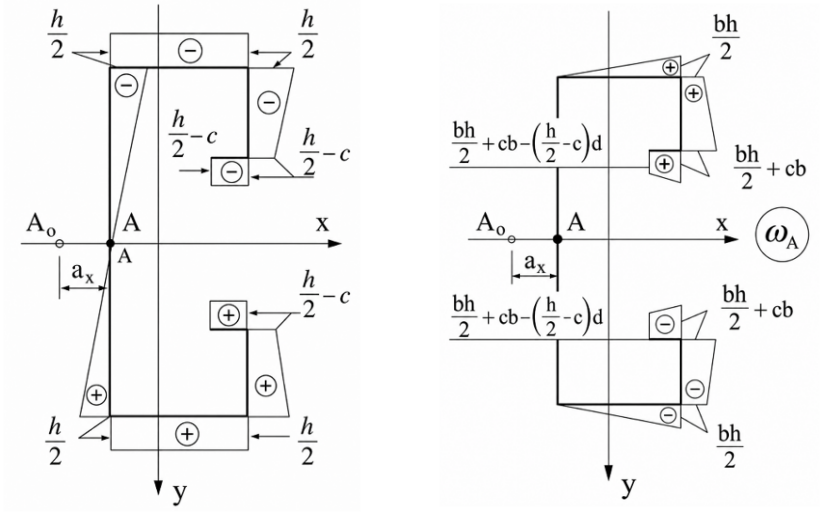
(a) Sectorial-coordinate points on the section

(b) Sectorial-coordinate diagram for the ILC section

Figure 8. Sectorial-coordinate diagram of the ILC section

Assume that point A is the origin, and that A_0 is the principal pole. Points 1 to 8 in Fig. 8(a) denote the sectorial coordinates at the corner locations of the section; the sectorial coordinates at these points are calculated as follows:

$$
\begin{aligned}
\omega_A &= 0 \\
\omega_1 &= -2.S_{\Delta A_0 A5} = -\frac{a_x h}{2} \\
\omega_2 &= \omega_1 + 2.S_{\Delta A_0 56} = -\frac{a_x h}{2} + \frac{bh}{2} = -\frac{h}{2}(a_x - b) \\
\omega_3 &= \omega_2 + 2.S_{\Delta A_0 67} = -\frac{h}{2}(a_x - b) + c(a_x + b) \\
\omega_4 &= \omega_3 + 2.S_{\Delta A_0 78} = -\frac{h}{2}(a_x - b) + c(a_x + b) - \left(\frac{h}{2} - c\right)d \\
\omega_5 &= 2.S_{\Delta A_0 A5} = \frac{a_x h}{2} \\
\omega_6 &= \omega_5 - 2.S_{\Delta A_0 56} = \frac{a_x h}{2} - \frac{bh}{2} = \frac{h}{2}(a_x - b) \\
\omega_7 &= \omega_6 - 2.S_{\Delta A_0 67} = \frac{h}{2}(a_x - b) - c(a_x + b) \\
\omega_8 &= \omega_7 - 2.S_{\Delta A_0 78} = \frac{h}{2}(a_x - b) - c(a_x + b) + \left(\frac{h}{2} - c\right)d
\end{aligned}
\tag{17}
$$



(a) y-ordinate diagram (b) Sectorial-coordinate diagram ω_A

Figure 9. Diagrams of the y-ordinate and the sectorial coordinate ω_A for the ILC section

d. Determination of the sectorial product of inertia $I_{\omega_A x}$ of the ILC section

According to Eq. (4), one obtains

$$
I_{\omega_A x} = \int_F \omega_A y dF = \int_F \omega_A y t ds = \sum_{i=1}^{7} t_i \int_0^{S_i} \omega_A y ds
$$

According to Vereshchagin's graphical multiplication method, after multiplying the ω_A and y diagrams in Fig. 9, one obtains:

$$I_{\omega_A x} = -2t\left(\frac{bh}{2}\frac{b}{2}\frac{h}{2}\right) - 2t\left[\frac{bh}{2}c\frac{h-c}{2} + \frac{cbc}{2}\left(\frac{h}{2} - \frac{2c}{3}\right)\right] - 2t\left[\frac{bh + 2cb - \left(\frac{h}{2} - c\right)d}{2}d\left(\frac{h}{2} - c\right)\right]$$

After simplifying the expression, one obtains

$$I_{\omega_A x} = -tb\left[\frac{bh^2}{4} + \frac{hc\,(h-c)}{2} + c^2\left(\frac{h}{2} - \frac{2c}{3}\right)\right] - td\left(bh + 2cb - \frac{hd}{2} + cd\right)\left(\frac{h}{2} - c\right) \tag{18}$$

e. Determination of the shear-center location of the ILC section

According to Eq. (7), the shear-center coordinates $A_0(x_{A_0}, y_{A_0})$ with a_x, a_y denoting the distances along the x- and y-axes between A and A_0 are obtained as follows:

$$a_x = \frac{I_{\omega_A x}}{I_x} \tag{19}$$

Because the x-axis is an axis of symmetry for the ILC section, one has $a_y = 0$.

f. Determination of the warping constant I_ω of the ILC section

According to Eq. (6), the warping constant of the ILC section is calculated as follows:

$$I_\omega = \int_F \omega^2 dF = \sum_{i=1}^{7} t_i \int_0^{S_i} \omega^2 ds$$

According to Vereshchagin's graphical multiplication method, after multiplying the diagram ω in Fig. 8(b) by itself and simplifying, one obtains the following formula:

$$I_\omega = 2t\left[\begin{array}{l} \dfrac{a_x^2 h^3}{24} + \dfrac{a_x^3 h^2}{12} + \dfrac{(b-a_x)^3 h^2}{12} + (c+d)\dfrac{h^2(b-a_x)^2}{4} \\ + \left(\dfrac{c}{2} + d\right)hc\,(a_x + b)\,(b - a_x) + \left(\dfrac{c}{3} + d\right)c^2(a_x + b)^2 \\ + \dfrac{d^3}{3}\left(\dfrac{h}{2} - c\right)^2 - \dfrac{hd^2}{2}\left(\dfrac{h}{2} - c\right)(b - a_x) - d^2 c\left(\dfrac{h}{2} - c\right)(a_x + b) \end{array}\right] \tag{20}$$

4. Numerical examples

This section presents numerical examples for calculating section properties and the critical load of concentrically compressed thin-walled members with OLC and ILC sections. The calculation of the critical buckling load shows how the derived geometric properties are directly used to verify member stability in engineering practice. The calculated results are compared with those obtained from CUFSM.

4.1. Outward-lipped channel section (OLC)

a. Calculation of section properties

Sections with combinations of geometric dimensions selected from the values given in Table 1, representating 7350 cases, are considered to validate the equations developed above.

As a specific example, based on the section dimensions provided by Global Storage Solutions [16], the comparison between the formulas and CUFSM of an OLC section equivalent to the P100 LT section, with dimensions $100 \times 50 \times 25 \times 25 \times 2$, is presented in Table 2.

Table 1. Geometric dimensions of the OLC section

Section geometric parameter	Value (mm)
h	[80; 100; 120; 140; 160; 180; 200]
b	[30; 40; 50; 60; 70; 80; 90]
c	[10; 15; 20; 25; 30]
d	[10; 15; 20; 25; 30]
t	[1.0; 1.2; 1.5; 2.0; 2.5; 3.0]

Table 2. Geometric properties of the OLC $100 \times 50 \times 25 \times 25 \times 2$ section and comparison between the analytical formulas and CUFSM

Section properties	Formula	CUFSM	Difference (%)
Shear center a_x (mm)	38.98364	38.98809	0.01142%
Warping constant I_ω (mm^6)	1729833226	1729833209	0.000001%

The remaining comparisions, were calculated similarly. The formula-based results were also compared with CUFSM using the shear center a_x and warping constant I_ω as the comparison parameter in Table 2. Based on the results in Table 2, the formula-based results and the CUFSM results are in very close agreement, with the maximum difference between the formula and the software equal to 0.048% for shear center and 0.000026% for warping constant. Therefore, the proposed formulas for calculating the geometric properties of the OLC section are reliable.

The formulas are then used to calculate the critical load of a concentrically compressed thin-walled member with an OLC section.

b. Calculation of the critical load of a concentrically compressed thin-walled member with an OLC section

Consider a pin-ended column with free warping at both ends, height $L = 1.5$ m, and section dimensions $100 \times 50 \times 25 \times 25 \times 2$, subjected to concentric compression. The material properties are $E = 205000$ N/mm^2, $G = 78846$ N/mm^2

Using the formulas in Section 3, the section properties are obtained as follows: $A = 600$ mm^2, $x_c = 27.08$ mm, $I_x = 875100$ mm^4, $I_y = 372495$ mm^4, $i_x = 38.19$ mm, $i_y = 24.92$ mm, $I_t = 800$ mm^4, $a_x = 38.98$ mm, and $I_w = 1729833226$ mm^6.

According to [11], the formulas for calculating the critical flexural-torsional buckling load of the member are as follows:

$$\begin{aligned} N_{cr,T} &= \frac{1}{i_0^2}\left(GI_t + \frac{\pi^2 EI_w}{L_{eT}^2}\right) \\ N_{cr,FT} &= \frac{N_{cr,x}}{2\beta}\left[1 + \frac{N_{cr,T}}{N_{cr,x}} - \sqrt{\left(1 - \frac{N_{cr,T}}{N_{cr,x}}\right)^2 + 4\left(\frac{x_0}{i_0}\right)^2 \frac{N_{cr,T}}{N_{cr,x}}}\right] \end{aligned} \tag{21}$$

where $\beta = 1 - \left(\frac{x_0}{i_0}\right)^2$, $N_{cr,x} = \frac{\pi^2 EI_x}{(KL)^2}$, $x_0 = a_x + x_C$, $i_0^2 = i_x^2 + i_y^2 + x_0^2$.

Substituting the calculated section properties, the critical flexural-torsional buckling load is obtained as:

$$x_0 = a_x + x_C = 66.06 \text{ mm}$$

$$i_0^2 = i_x^2 + i_y^2 + x_0^2 = 6444.17;\ i_0 = 80.27 \text{ mm}$$

$$\beta = 1 - \left(\frac{x_0}{i_0}\right)^2 = 0.323$$

$$N_{cr,x} = \frac{\pi^2 E I_x}{(KL)^2} = 786916.7 \text{ N}$$

$$N_{cr,T} = \frac{1}{i_0^2}\left(GI_t + \frac{\pi^2 E I_w}{L_{eT}^2}\right) = 251172.06 \text{ N}$$

$$N_{cr,FT} = \frac{N_{cr,x}}{2\beta}\left[1 + \frac{N_{cr,T}}{N_{cr,x}} - \sqrt{\left(1 - \frac{N_{cr,T}}{N_{cr,x}}\right)^2 + 4\left(\frac{x_0}{i_0}\right)^2 \frac{N_{cr,T}}{N_{cr,x}}}\right] = 203.2 \text{ kN}$$

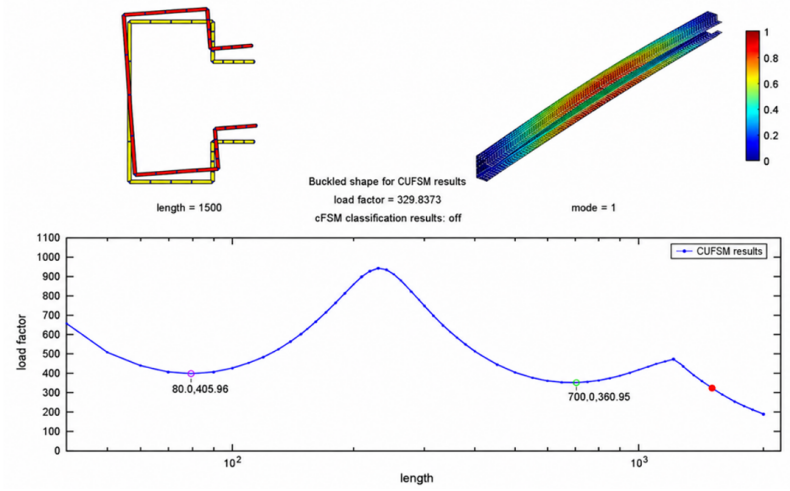
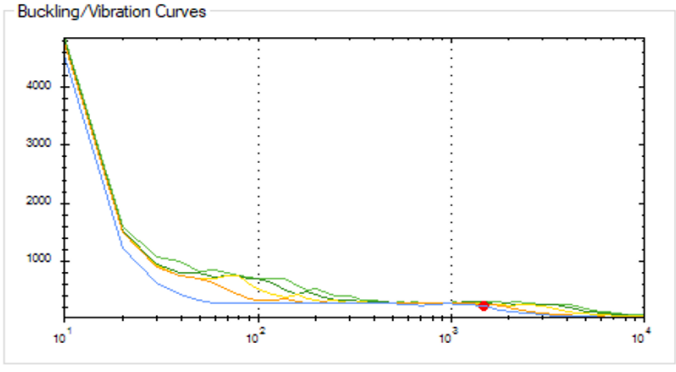


Figure 10. Flexural-torsional buckling analysis of the OLC section using CUFSM



Results of the buckling analysis of the member with L=1500 (Mode 1)

Buckling Load: Pb = 199.64958

Modal participations (%) of the most important GBT modes:

P4=77.57 P2=20.43 P6=1.96 Other=0.04

Figure 11. Flexural-torsional buckling analysis of the OLC section using GBTUL

Using CUFSM, the flexural-torsional buckling analysis of the member gives the critical buckling stress $\sigma_{cr} = 329.83$ N/mm^2 in Fig. 10, and the corresponding critical flexural-torsional buckling load is $N_{cr} = A \cdot \sigma_{cr} = 197.9$ kN.

In addition, GBTUL [17] is used to analyze global buckling of the section, giving $N_{cr} = 199.6$ kN, as shown in Fig. 11.

These results show that the difference between the formula-based calculation and the software analysis is 2.7% relative to CUFSM and 1.8% relative to GBTUL.

4.2. Inward-lipped channel section (ILC)

a. Calculation of section properties

Sections with combinations of geometric dimensions selected from the values given in Table 1 are considered.

For an ILC section with dimensions $100 \times 50 \times 25 \times 25 \times 2$, the formula-based results and the software results are presented in Table 3.

Table 3. Geometric properties of the ILC $100 \times 50 \times 25 \times 25 \times 2$ section and comparison between the analytical formulas and CUFSM

Section properties	Formula	CUFSM	Difference (%)
Shear center a_x (mm)	37.19813	37.20238	0.014%
Warping constant I_ω (mm^6)	1380130844	1380130828	0.0000011%

The remaining comparisions, were calculated similarly. The formula-based results were also compared with CUFSM using the shear center a_x and warping constant I_ω as the comparison parameter in Table 3. Based on the results in Table 3, the formula-based results and the CUFSM results are in very close agreement, with the maximum difference between the formula and the software equal to 0.048% for shear center and 0.000031% for warping constant. Therefore, the proposed formulas for calculating the geometric properties of the ILC section are reliable.

The formulas are then used to calculate the critical load of a concentrically compressed thin-walled member with an ILC section.

b. Calculation of the critical load of a concentrically compressed thin-walled member with an ILC section

Consider a pin-ended column with free warping, height $L = 1.6$ m, and section dimensions $100 \times 50 \times 25 \times 25 \times 2$, subjected to concentric compression. The material properties are $E = 205000$ N/mm^2, $G = 78846$ N/mm^2.

Using the formulas in Section 3, the section properties are obtained as follows: $A = 600$ mm^2, $x_c = 22.92$ mm, $I_x = 875100$ mm^4, $I_y = 247495$ mm^4, $i_x = 38.19$ mm, $i_y = 20.31$ mm, $I_t = 800$ mm^4, $a_x = 37.19$ mm, and $I_w = 1380130844$ mm^6.

According to [11], the formulas for calculating the critical flexural-torsional buckling load of the member are analogous to Eq. (21):

Substituting the calculated section properties, the critical flexural-torsional buckling load is obtained as:

$$x_0 = a_x + x_C = 60.11 \text{ mm}$$

$$i_0^2 = i_x^2 + i_y^2 + x_0^2 = 5484.78 \text{ mm}^2; \; i_0 = 74.06 \text{ mm}$$

$$\beta = 1 - \left(\frac{x_0}{i_0}\right)^2 = 0.341$$

$$N_{cr,x} = \frac{\pi^2 EI_x}{(KL)^2} = 691626 \text{ N}$$

$$N_{cr,T} = \frac{1}{i_0^2}\left(GI_t + \frac{\pi^2 EI_w}{L_{eT}^2}\right) = 210372.7 \text{ N}$$

$$N_{cr,FT} = \frac{N_{cr,x}}{2\beta}\left[1 + \frac{N_{cr,T}}{N_{cr,x}} - \sqrt{\left(1 - \frac{N_{cr,T}}{N_{cr,x}}\right)^2 + 4\left(\frac{x_0}{i_0}\right)^2 \frac{N_{cr,T}}{N_{cr,x}}}\right] = 172.6 \text{ kN}$$

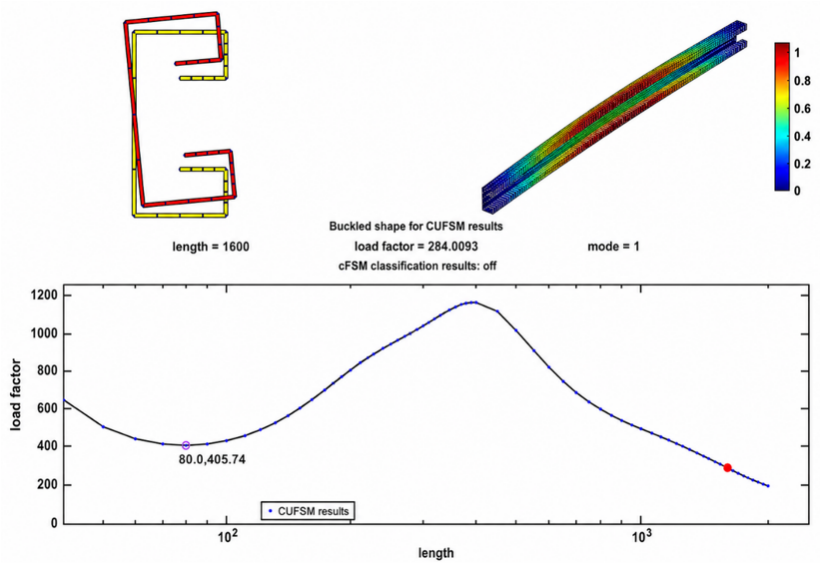
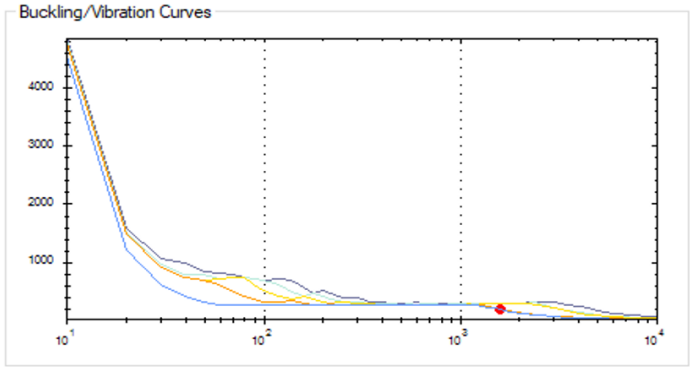


Figure 12. Flexural-torsional buckling analysis of the ILC section using CUFSM



Results of the buckling analysis of the member with L=1600 (Mode 1)

Buckling Load: Pb = 171.7179

Modal participations (%) of the most important GBT modes:

P4=80.38 P2=19.07 P8=0.35 Other=0.2

Figure 13. Flexural-torsional buckling analysis of the ILC section using GBTUL

Using CUFSM, the flexural-torsional buckling analysis of the member gives the critical buckling

stress σ_{cr} = 284.01 N/mm^2 in Fig. 12, and the corresponding critical flexural-torsional buckling load is $N_{cr} = A \cdot \sigma_{cr}$ = 170.4 kN.

In addition, GBTUL is used to analyze global buckling of the section, giving N_{cr} = 171.7 kN, as shown in Fig. 13.

These results show that the difference between the formula-based calculation and the software analysis is 1.3% relative to CUFSM and 0.5% relative to GBTUL.

5. Conclusions

This paper presented the theoretical basis for calculating the geometric properties of storage rack columns, treated as open-section thin-walled members. The calculation includes the determination of the shear-center location, the sectorial-coordinate diagram and the warping constant. The paper also demonstrated the procedure used to establish closed-form formulas for two complex section types, namely OLC and ILC. These formulas simplify and increase the flexibility of critical load calculations for members without requiring supporting software.

The numerical examples demonstrated the high reliability of the proposed formulas and highlighted the role of geometric properties in structural design calculations. The results also showed that the critical global buckling load obtained from CUFSM is lower than those obtained from GBTUL and from the standard-based formulas, which is consistent with the assumptions of Vlasov theory. It should be noted that this study focuses on the gross cross-section without perforations. In practice, storage rack columns usually contain regular holes, which reduce their geometric properties. Therefore, studying the effect of perforations and developing reduction factors will be an important focus of our future research. On this basis, the method can be further developed for members with more complex cross sections and for other applications related to storage rack column systems.

Declaration of generative AI and AI-assisted technologies

During the preparation of this manuscript, the authors used Gemini strictly for language editing and proofreading, with no changes made to the research findings. The authors reviewed all edited draft and take full responsibility for the content and integrity of the publication.

References

[1] Schafer, B. W., Adany, S. (2006). Buckling analysis of cold-formed steel members using CUFSM: Conventional and constrained finite strip methods. In *Eighteenth International Specialty Conference on Cold-Formed Steel Structures*, Orlando, Florida, 18:39–54.

[2] Nguyen, V. V., Hancock, G. J., Pham, C. H. (2015). Development of the Thin-Wall-2 Program for buckling analysis of thin-walled sections under generalised loading. In *International Conference on Advances in Steel Structures*, Lisbon, Portugal, ICASS, 8.

[3] Cuong, B. H. (2010). Calculation of geometric properties of open thin-walled member sections. *Journal of Science and Technology in Civil Engineering (STCE) - HUCE*, 4(2):16–28. (in Vietnamese).

[4] Xiang, C., Seaburg, P. A., Crain, R., Lou, A. C. J. (2002). On the computation of the cross-section properties of arbitrary thin-walled structures. In *Sixteenth International Specialty Conference on Cold-Formed Steel Structures*, 16(9):602–615.

[5] American Iron and Steel Institute (2003). *AISI Manual cold-formed steel design 2002 edition*. AISI Specifications for the Design of Cold-Formed Steel Structural Members.

[6] Vlasov, V. Z. (1961). *Thin-walled elastic beams*. Israel Program for Scientific Translation, Jerusalem.

[7] Gil-Martín, L. M., Hernández-Montes, E. (2020). Principal sectorial coordinate system. *Archive of Applied Mechanics*, 90(2):305–312.

[8] Lue, D., Liu, J.-L., Lin, C.-H. (2007). Numerical evaluation on warping constants of general cold-formed steel open sections. *International Journal of Ssteel Structures*, 7(4):297–309.

[9] Shama, M. (2011). Sectorial properties of thin-walled open sections. In *Torsion and shear stresses in ships*, Berlin, Heidelberg, Springer, page 91–104.

[10] Freitas, A. M. S., Freitas, M. S. R., Souza, F. T. (2005). Analysis of steel storage rack columns. *Journal of Constructional Steel Research*, 61(8):1135–1146.

[11] BS EN 15512:2020 (2021). *Steel static storage systems. Adjustable pallet racking systems - Principles for structural design*.

[12] Quyen, V. L. (2023). Constrained torsion analysis of open-section thin-walled members. *Construction Journal*, 7:42–45. (in Vietnamese).

[13] Tuyen, N. M., Cuong, B. H. (2015). Calculation of geometric properties of closed thin-walled sections subjected to torsion. *Journal of Science and Technology in Civil Engineering (STCE) - HUCE*, 9(3): 43–51. (in Vietnamese).

[14] Tung, V. S., Cuong, B. H. (2017). Effect of welded built-up I-section beam with hollow flange. *Science Journal of Architecture & Construction*, 27:54–56. (in Vietnamese).

[15] EN 1993-1-3 (2006). *Eurocode 3: Design of steel structures - Part 1-3: General rules - Supplementary rules for cold-formed members and sheeting*. European Committee for Standardization (CEN).

[16] Global Storage Solutions. *Pallet racking - P90 standard details*. Accessed on 06 May 2026.

[17] Bebiano, R., Camotim, D., Gonçalves, R., Silvestre, N. (2018). GBTUL 2.0 – A second-generation code for the GBT-based buckling and vibration of thin-walled members. *Thin-Walled Structures*, 124:235–257.